利用T型閘極與氨氣電漿處理提升薄膜電晶體元件可靠度之研究

研究生： 蔣陳偉　　　　　　　　　　指導教授： 葉清發 博士

國立交通大學電子工程學系　　電子研究所碩士班

摘要

複晶矽薄膜電晶體對於應用在液晶顯示器上能夠有效的減少面積且提升顯示器之解析度，且複晶矽薄膜電晶體相較於非晶矽而言有較大的載子遷移率，所以利用複晶矽薄膜電晶體可以將周邊電路整合在玻璃基板上來降低成本，但是對於複晶矽薄膜電晶體卻有較大的漏電流，而使的元件的功率損耗很嚴重。對於複晶矽薄膜電晶體其漏電主要與缺陷密度和集極電場強度有關，在本篇論文中我們發現氮化矽絕緣層能夠有效的阻擋氫原子向下擴散而累積在通道之中，更進一步的去修補通道中的缺陷。因此我們利用此種特性設計了氮化矽緩衝層的薄膜電晶體結構來增加電將處理的修補效率，我們也比較了長時間電漿處理對於傳統薄膜電晶體結構和氮化矽緩衝層的薄膜電晶體結構的差異。

傳統的複晶矽薄膜電晶體結構會因為較高的汲極電場而導致有較高的漏電流和熱電子可靠的的問題，因此我們利用選擇性液相沉積來製作自我對準的T型閘極結構的複晶矽薄膜電晶體，用來降低汲極端的側向電場來有效的降低漏電。同時 kink 的效應也明顯的降低和熱載子的可靠度也明顯的提升，然後我們也研究T型閘極的結構和一般傳統結構對於電漿處理後的差異。

Improving Reliability Characteristics of Thin Film Transistors by T-gate Structure and NH_3 Plasma Passivation

Student: Chen-Wei Chiang Advisor: Dr. Ching-Fa Yeh

Department of Electronics Engineering &

Institute of Electronics

National Chiao Tung Unversity

Abstract

Application of polycrystalline silicon thin-film transistors (poly-Si TFTs) in large area active-matrix liquid-crystal displays (AMLCDs) can effectively improve resolution and reduce the export area, and poly-Si TFTs have higher field effect mobility than α-Si. That the poly-Si can integrate the peripheral circuit in glass substrate and reduce cost. Currently, the anomalous leakage current was major problem for poly-Si TFTs then increase the power consumption. The leakage current of poly-Si TFTs is owing to the high drain electric field and large trap state density at drain junction. In this thesis, we found the silicon nitride film as the diffusion barrier prevents the hydrogen atoms downward diffusion and accumulated at the channel to further reduce the trap state density. We developed the buffer nitride layer poly-Si thin film transistor to increase the passivation efficiency. We also compare the device characteristics of conventional TFTs and buffer nitride layer TFTs for long time plasma passivation.

The conventional poly-Si thin film transistors have large leakage current and poor hot carrier endurance at high drain electric field. So we using the selective liquid phase deposition technique to fabricate the self-align T-gate poly-Si thin film transistors. The T-gate structure can reduce the drain side lateral electric field and decrease the off-state leakage current. It also release the impact ionization effect so that the kink effect to been suppressed and improve the

hot carrier endurance. Finally, we compare the conventional thin film transistors and T-gate thin film transistor characteristic for plasma passivation effect.

Acknowledgment

感謝羅正忠老師在這兩年內細心的指導，使我在碩士的研究過程中獲得很大的幫助也讓我能順利的畢業。非常謝謝葉清發老師讓我在交通大學的兩年內不僅在學業上受益良多，在待人處世和做人做事的道理有了更進一步的了解。更要感謝王碩晟、陳添富和劉俊彥學長，在實驗的想法和過程中給予的幫助使我做起實驗更有效率。

其次，我要感謝交通大學電子研究所這兩年來的栽培，系所老師們的認真教學使身為學生的我終身受用不盡。另外，我要感謝國家奈米實驗中心（NDL）和交通大學奈米中心的研究員及設備工程師們，由於你們的協助使我能在一流的製程設備中從事我的研究工作。

感謝 Yeh's groups 中蕭智文、林榮祥學長們的指導與協助。感謝陳昶維、施俊宏、鍾漢邠、吳伯慶、洪啓哲、陳彥廷、許雁雅、張佑慈等同學在實驗過程中的互相鼓勵及協助，我想大家一定會懷念那段一起唸書與作實驗時光。

最後，我要感謝我的父母親－蔣光輝先生與陳淑慧女士以及姐姐蔣欣怡在我求學及從事研究過程中給我的最大的支持與關心，使我能在兩年的時光中順利完成我的學業，謝謝你們。

Contents

Chinese Abstract i
English Abstract ii
Acknowledgment iv
Contents v
Table Captions vii
Figure Captions viii

Chapter 1 Introduction

1.1 General Background and Motivation 1
1.2 Organization of This Thesis 3

Chapter 2 NH_3 Plasma Treatment on the Electrical Characteristics of Poly-Si Thin Film Transistors

2.1 Introduction 4
2.2 Experiment Details
2.2.1 Fabrication of bottom-gated poly-Si TFTs 4
2.2.2 Fabrication of conventional poly-Si thin film transistors and buffer nitride thin film transistors 6
2.2.3 Sample for SIMS analysis sample 8
2.3 Results and Discussions
2.3.1 Leakage current mechanism for poly-Si TFTs 9
2.3.2 Hydrogenation effect on bottom gate TFTs 10
2.3.3 Hydrogenation effect on buffer nitride layer TFTs 11
2.3.4 Long-time NH_3 plasma treatment on threshold voltage and subthreshold swing 13
2.3.5 Long-time NH_3 plasma treatment on field effect mobility and ON current... 13
2.4 Summary 15

Chapter 3 Characteristics of T-gate Poly-Si Thin Film Transistors

3.1 Introduction 42

3.2 Experiments for Long-time NH_3 Plasma Treatment

3.2.1 Fabrication of conventional poly-Si TFTs and T-gate poly-Si TFTs 43

3.2.2 Selective liquid phase deposition 44

3.3 Results and Discussions

3.3.1 Electrical characteristics of T-gate poly-Si thin film transistors 45

3.3.2 Threshold voltage and subthreshold swing characteristic of T-gate poly-Si TFTs 46

3.3.3 Off-sate current and kink effect reduction 47

3.3.4 Hot carrier endurance 48

3.3.5 NH_3 plasma passivation effect 48

3.4 Summary 49

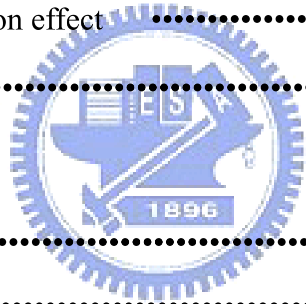

Chapter 4 Conclusions

4.1 Conclusions 71

4.2 Future Works 72

References 74

Publications 78

Vita 79

Table Captions

Table 2.1 The electrical characteristics of bottom-gated poly-Si TFTs before and after NH_3 plasma hydrogenation.

Table 2.2 The electrical characteristics of Top-gate poly-Si TFTs before and after NH_3 plasma hydrogenation.

Table 3.1 The electrical characteristics of CTFTs and TGTFTs before plasma treatment.

Table 3.2 The electrical characteristics of CTFTs and TGTFTs after plasma treatment.

Figure Captions

Chapter 2

Figure 2.1 Process flows of p-type bottom-gated poly-Si TFTs.

Figure 2.2 Process flows of n-type buffer nitride layer poly-Si TFTs.

Figure 2.3 Process flows of SIMS analysis sample.

Figure 2.4 Schematic illustration of the leakage current model in poly-Si TFTs.

Figure 2.5 (a) Transfer characteristics for comparison of p-type bottom-gated TFTs before and after hydrogenation at V_{DS}= -0.1 V. Sample A (gate oxide), and B (gate nitride) treat 360 min, and 300min NH_3 plasma passivation.

Figure 2.5 (b) Transfer characteristics for comparison of p-type bottom-gated TFTs before and after hydrogenation at V_{DS}= -5 V. Sample A (gate oxide), and B (gate nitride) treat 360 min, and 300min NH_3 plasma passivation.

Figure 2.6 (a) The SIMS profiles of SiN for SiO_2 and Si_3N_4 with 480 min NH_3 plasma treatment.

Figure 2.6 (b) The SIMS profiles of hydrogen concentration for SiO_2 and Si_3N_4 with 480 min NH_3 plasma treatment

Figure 2.7 (a) Transfer characteristics for comparison of BNTFTs with and Without SiO layer at V_{DS} = 0.1V and 5V, respectively.

Figure 2.7 (b) Transfer characteristics for comparison of BNTFTs and CTFT pretreatment effect.

Figure 2.8 (a) Transfer characteristics for comparison of BNTFTs and CTFT before and after hydrogenation at V_{DS}= 0.1 V.

Figure 2.8 (b) Transfer characteristics for comparison of BNTFTs and CTFT before and after hydrogenation at V_{DS}= 5 V.

Figure 2.9 Transfer characteristics for comparison of NBTFTs and CTFT before hydrogenation at V_{DS}= 0.1 V.

Figure 2.10 (a) Threshold voltage as function of NH3 plasma passivation time for W = 20 µm and L = 8 µm BNTFTs.

Figure 2.10 (b) Subthreshold swing as function of NH3 plasma passivation time for W = 20 μm and L = 8 μm BNTFTs.

Figure 2.11 (a) Field effect mobility as function of NH3 plasma passivation time for W = 20 μm and L = 8 μm NBTFTs.

Figure 2.11 (b) ON-state current as function of NH3 plasma passivation time for W = 20 μm and L = 8 μm NBTFTs.

Figure 2.12 (a) Subthreshold swing as function of NH3 plasma passivation time for W = 20 μm and L = 2,5 μm p-type bottom-gate TFTs.

Figure 2.12 (b) Threshold voltage as function of NH3 plasma passivation time for W = 20 μm and L = 2,5 μm p-type bottom-gate TFTs.

Figure 2.13 Field effect mobility as function of NH3 plasma passivation time for W = 20 μm and L = 2 μm p-type bottom-gate TFTs.

Figure 2.14 (a) The pathway for hydrogen migration from a gaseous source to the active channel region of a bottom-gate TFT

Figure 2.14 (b) The pathway for hydrogen migration from a gaseous source to the active channel region of a top-gate BNTFT.

Figure 2.15 (a) Cumulative distribution of Field effect mobility before and after plasma treatment for CTFTs and NBTFTs.

Figure 2.15 (b) Cumulative distribution of ON-state current before and after plasma treatment for CTFTs and NBTFTs..

Figure 2.16 cumulative distribution of Threshold voltage before and after plasma treatment for CTFTs and BNTFTs.

Chapter 3

Figure 3.1 Possible pathways for hydrogen migration from a gaseous source to the active channel region of a top-gated poly-Si TFT structure.

Figure 3.2 Key process flows of the bottom-gated poly-Si TFTs using SPC processes.

Figure 3.3 Key process flows of the top-gated poly-Si TFTs using SPC/ELA processes.

Figure 3.4 Subthreshold Swing determined at V_{DS}= -0.1V as function of NH_3 plasma passivation time for W= 10μm and L= 2 μm p-type bottom-gated poly-TFTs

Figure 3.5 (a) Threshold voltage determined at V_{DS}= -0.1V as function of NH_3 plasma passivation time for W= 20μm and L= 5 μm p-type bottom-gated poly-TFTs.

Figure 3.5 (b) Threshold voltage determined at V_{DS}= -0.1V as function of NH_3 plasma passivation time for W= 20μm and L= 5 μm p-type top-gated poly-TFTs.

Figure 3.5 (c) Threshold voltage determined at V_{DS}= -0.1V as function of NH_3 plasma passivation time for W= 20μm and L= 10μm n-type poly-TFTs.

Figure 3.6 (a) Mobility determined at V_{DS}= -0.1V as function of NH_3 plasma passivation time for W= 10μm and L= 2 μm p-type bottom-gated poly-TFTs.

Figure 3.6 (b) Mobility determined at V_{DS}= -0.1V as function of NH_3 plasma passivation time for W= 20μm and L= 10 μm p-type top-gated poly-TFTs.

Figure 3.6 (c) Mobility determined at V_{DS}= 0.1V as function of NH_3 plasma passivation time for W= 20μm and L= 5 μm n-type poly-TFTs.

Figure 3.7 (a) The leakage currrent determined at V_{DS}= -5V as function of NH_3 plasma passivation time for W= 10μm and L= 2 μm p-type bottom-gated poly-TFTs.

Figure 3.7 (b) The leakage currrent determined at V_{DS}= -5V as function of NH_3 plasma passivation time for W= 20μm and L= 10 μm p-type top-gated poly-TFTs.

Figure 3.8 (a) Effective trap density determined at V_{DS}= -0.1V as function of NH_3 plasma passivation time for W= 20μm and L= 5 μm p-type bottom-gated poly-TFTs.

Figure 3.8 (b) Effective trap density determined at V_{DS}= -0.1V as function of NH_3 plasma passivation time for W= 20μm and L= 2 μm p-type top-gated poly-TFTs.

Chapter 4

Figure 4.1 A new structure of combine the buffer nitride layer and the T-gate structure poly-Si TFTs

Figure 4.2 A new structure of T-gate poly-Si TFTs with lightly doped drain.